2009 International Conference on Artificial Intelligence and Computational Intelligence

Effect of training artificial neural networks on 2D image: An example study on mammography

Xuejun Zhang, Hiroshi Fujita, Jing Chen and Zuojun Zhang

Xuejun Zhang, and Jing Chen
Department of Electronics and Information Engineering, School of Computer, Electronics and Information
Guangxi University
Nanning City, Guangxi 530004, P. R. China
e-mail: xjzhang@gxu.edu.cn, chenjing@mail.gxu.cn

Hiroshi Fujita
Department of Intelligent Image Information, Division of Regeneration and Advanced Medical Sciences
Graduate School of Medicine, Gifu University
Gifu City, Gifu 501-1194, Japan
e-mail: fujita@fjt.info.gifu-u.ac.jp

***Abstract*—Several structures of artificial neural networks (ANNs) with different training patterns were investigated so as to compare their performances on detecting the cluster of microcalcifications (CM) on mammography. 150 region-of-interests (ROIs) around mass containing both positive and negative microcalcifications were selected for training the network by a standard or modified error-back-propagation algorithm. A rule-based triple-ring filter (TRF) was used for evaluating the performances of these two different types of methods. The results showed that the shift-invariant artificial neural network (SIANN) was the best ANN model to detect CM, while SIANN and TRF had different ability of detecting microcalcifications. In a practical detection of 30 cases with 40 clusters in masses, the sensitivity of detecting CMs was improved from 90% by our previous method to 95% by using both SIANN and TRF.**

Keywords- mammogram; microcalcification; mass; artificial neural network; triple-ring filter analysis; computer-aided diagnosis (CAD)

I. INTRODUCTION

Microcalcifications are often the first and sometimes the only radiographic findings in early, curable breast cancers [1]. Furthermore, the existence of a cluster of microcalcifications (CM) in mass on mammograms is one of important features for distinguishing the breast cancer between benign and malignant. However, it often fails to be detected because of its low subject contrast in denser background and small quantity of microcalcifications. To assist radiologists in detecting clustered microcalcifications on mammograms, a number of research groups have attempted to analyze mammographic abnormalities with digital computers [2, 3]. An automated computerized scheme based on triple-ring filter and feature extraction techniques had been developed by our group [4]. We also applied a conventional artificial neural network (ANN) to improve the detection performance [5]. However, the issue to be solved was to efficiently detect the CMs in mass area with least number of false positives (FPs). Several structures of ANNs with different training patterns were investigated in this experiment so as to compare their performances on detecting the CMs on mammography. The shift-invariant artificial neural network (SIANN) had been shown to be a powerful tool to eliminate over half of FP clusters without any loss of the true-positive (TP) clusters [6]. In this work, we combined the SIANN with TRF method in our CAD system to get a higher performance of detecting clusters in mass area, and other two conventional ANNs were also discussed in this paper. Although there are many papers combining image manipulation filters with neural networks, or using RBF networks [7, 8] instead of BP [9], our paper focus on the different effects by training with various patterns using a same training method rather than trying different approaches.

II. MATERIALS AND METHODS

2.1Case selection

40 cases with clusters in mass were selected from the database at Aichi Cancer Center Hospital in Japan. Digitized mammograms with a pixel size of 0.1 mm in 10 bits were

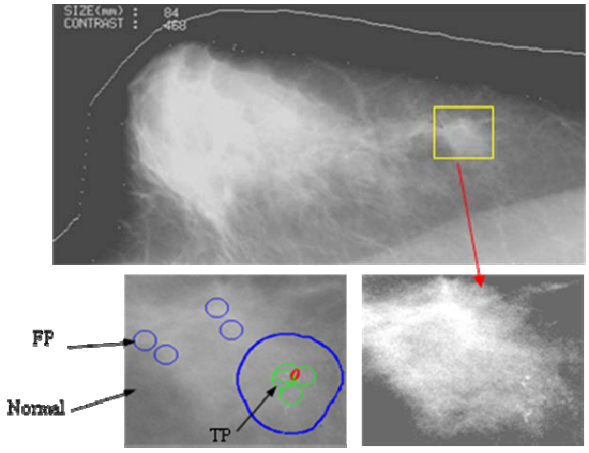

Fig. 1 A mammographic image with a mass area (square) that contains a cluster of microcalcifications. TP: true-positive cluster of microcalcifications, FP: false-positive cluster of microcalcifications. Normal: normal tissues.

978-0-7695-3816-7/09 $26.00 © 2009 IEEE
DOI 10.1109/AICI.2009.475

used for detecting microcalcifications, and the compressed 0.4-mm-pixel-size images were employed for extracting mass candidates in our CAD scheme [10]. All the images were normalized by contrast correction from heterogeneous background as shown in Fig. 1.

2.2 Artificial Neural Network and Its Architecture

Artificial neural network (ANN) is a structure of simulated neurons that are connected together somewhat in the same way as natural neurons are thought to be connected in the brain. The capability and advantages of ANNs are due to their special features including nonlinear, adaptive, and parallel processing. Each neuron of ANNs receives inputs either from a number of other neurons or from an external stimulus. The weighted sum of these inputs passes through a basis function and the resulted argument is applied to an activation function that finally yields the outputs of the neurons. The manner in which connections are made between these neurons (viz. the topology) defines the flow of information in the network and is called the architecture of the network. Useful architectural configurations include single layer, multilayer, feed-forward, feedback and lateral connectivity. Indeed, it is relatively straightforward to build an ANN model from input–output data. Behavior of a network depends greatly on the interactions between these building blocks. There are three types of neuron layers: input, hidden, and output layers. The more the layers are used, the greater the power the network possesses will be. On the other hand, an excessive number of layers often appear to be counter- productive. It may cause slower convergence in the back-propagation learning. Generally speaking, three-layer network could be adequate as a universal approximator of any nonlinear function.

In this research, we develop several structures of artificial neural networks so as to compare their performances on detecting the CM in mass area.

2.2.1 ANN for classification of microcalcification

ANN model has been proven to be very effective in solving the problem of classification in medical images [11, 12]. The architecture of this ANN is that of a totally connected layered feed-forward network with only one output unit, where the input units are the normalized pixel values from 2D images corresponding to the time and frequency domains. Figure 2 shows that a three-layer feed-forward neural network contained an input layer with 121 units, one hidden layer with 60 units, and one output layer with 1 unit. A region-of-interest (ROI) with input size 11*11 contains a microcalcification so-called true positive (TP) or gland tissue so-called false positive (FP) with its center of gravity in the middle of ROI, and each input unit is scaled to a numerical value from 0 to 1 that is proportional to the gray value of a pixel after contrast correction. Each node in layer X (where X=0 means inputs, X=1 means first hidden layer of units, etc.) is connected to all the units in layer X+1.

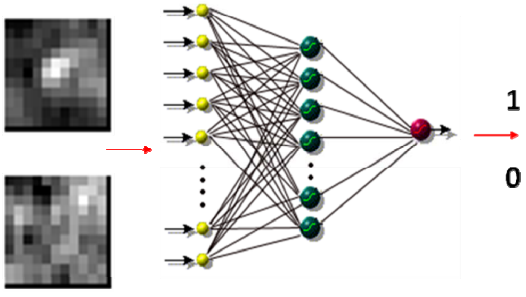

Fig. 2 ANN for classification of microcalcification contained an input layer with 121 units, one hidden layer with 60 units, and an output layer with 1 unit.

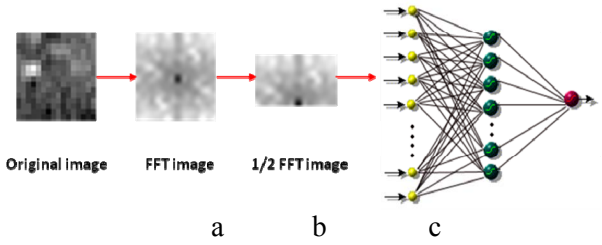

Fig. 3 A structure of FFT-ANN with Input Layer=128 units, Hidden Layer=64 units and Output Layer=1 unit.

An error back-propagation (EBP) algorithm [9] with generalized delta rule was used to train the neural network. A unit in the output layer is 1, only if the units in the input layer have a microcalcification at the center of ROI, otherwise is 0. The input values of ANN can be selected not only from spatial domain but also frequency domain. A Fast Fourier transformation (FFT) is applied to calculate the power spectra of a 2D image (a) as shown in Fig.3, from which its visualized spectra image (b) is symmetric about the origin, therefore only one half of the spectra (c) is needed. The power spectra is converted using a logarithmic scale to reduce the dynamic range of the data.

2.2.2 ANN for detection of microcalcification

In an actual scanning by a ROI on mammographic images for searching a microcalcification, the position of a microcalcification is not always at the center of ROI. Therefore, the output is designed to be able to indicate the location of TP microcalcification as shown in Fig. 4. This feed-forward neural network contained an input layer with

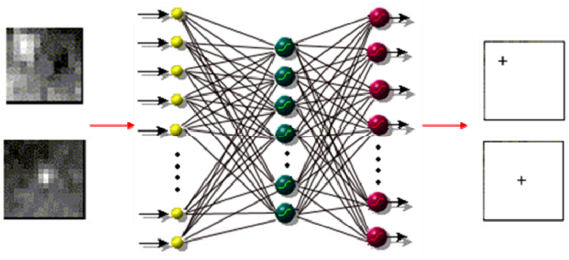

Fig. 4 ANN for detecting microcalcification with Input Layer=121 units, Hidden Layer=60 units and Output Layer=121 units; + means the output is 1, the others are 0.

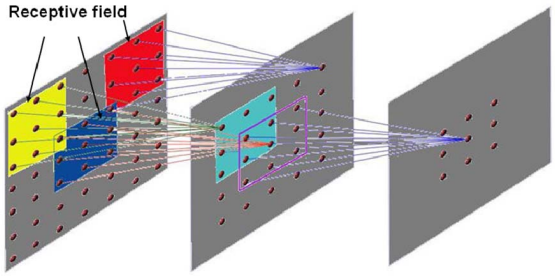

Fig. 5 Example of a three-layer shift-invariant network connection with receptive size=3, group=1, Input Layer=7x7 units, Hidden Layer=5x5 units and Output Layer= 3x3 units.

121 units, one hidden layer with 60 units, and an output layer with 121 units. A unit in the output layer is 1, only if the corresponding unit in the input layer is at the center of a microcalcification, otherwise is 0.

2.2.3 ANN for detecting clustered microcalcification

In a practical inspection of breast cancers, the existence of a cluster of microcalcifications is one of important features for distinguishing the breast cancer between benign and malignant. Therefore, to detect CMs is much more useful than individual microcalcification in clinic.

2.2.3.1 Conventional full-connected neural network

The structure of ANN used in section 2.2.1 and 2.2.2 is modified for detecting CMs with a ROI size change to 21x21. 2D image inputs are calculated both in spatial domain and frequency domain, and the output of ANN is regarded as a CM if an input ROI contains over 3 microcalcifications.

2.2.3.2 The shift-invariant neural network

Since back-propagation (BP) algorithm was introduced in 1985, there have been many variations attempted, with the aim of making it run faster and less likely to become stuck in local minima. A shift-invariant artificial neural network had been described by Zhang et al. [6], which was a layered feed-forward neural network with local interconnections as illustrated in Figure 5. The basic structure of the SIANN was similar to that of the Neocognitron model developed by Fukushima et al.[13], which was quite successfully applied to the handwriting recognition. However, the SIANN was a feed-forward neural network trained with EBP. Though the architecture looks like a standard 3-layer BP network, there is a crucial difference: the hidden units embody a different type of neurons altogether. These units have a receptive field: that is, they have their maximal response (generally 1) for some particular point in the input space, and this response tails off as the input value moves away from this point. As shown in Fig. 5, units in the input layer and output layer corresponding to pixels of the input and output were divided into groups. Every unit in a subsequent layer was connected with the units of a small region called the receptive field in every group in the preceding.

2.3 Training methods and datasets

It has long been known that general networks of units provided a much richer computation capacity. But without the applicable learning methods, the ANN could not work as our expectation. The numbers of input patterns selected teacher signal and how they are arranged are crucial to the training procedure. In this experiment we selected 150 region-of-interests (ROIs) around mass containing both positive and negative microcalcifications for training the network, as well as the same populations of CM datasets. Another 30 cases were selected for testing the trained ANN.

For the conventional full-connected neural network, ANN is trained by use of the well-known backpropagation (BP) algorithm [9]. The selection of hidden layer units is decided by the complexity of the case data. If the number of units is less than half of the input units, the learning procedure of the ANN becomes slow and convergence is difficult, and it results in failure of learning CM teacher signal even in the training dataset. Therefore, we selected 60 or more hidden units in the ANN used in section 2.2.1 and 2.2.2. The network learning rate was set to 0.9, momentum factor 0.3, and the number of training iterations was always at 5000 to 7000, with a 100% training accuracy.

A back-propagation algorithm with a generalized delta rule was modified to train the neural network with the shift-invariant-connection constraint, and the sigmoid function was used as the activation function for each processing unit in the neural network. In the training process, the internal parameters of the connections between layers were adjusted iteratively so that the difference between the output values and the desired results was minimized. The training was stopped at 6,000 iterations to avoid overtrained problem. The SIANN was trained by an improved error back-propagation algorithm [6] with a 21x21-17x17-13x13 structure.

The ANN's ability to detect microcalcifications was assessed using receiver operating characteristic (ROC) analysis to calculate the area under the ROC curve (AUC) and the results were compared with a logistic rule-based triple-ring filter (TRF) model, which was a particular cone-shaped vector pattern detector by calculating the features from direction and magnitude of the gradient vector [4].

III. RESULTS AND DISCUSSION

The consistency test indicated that the neural networks for the classification and detection of single microcalcification are able to learn all of the 150 patterns that were used for the training.

For the classification of microcalcification by the ANN in Fig. 2, when the microcalcification is located at the center of ROI, the output value of ANN is very high, while with the shifting position of microcalcification, its output becomes

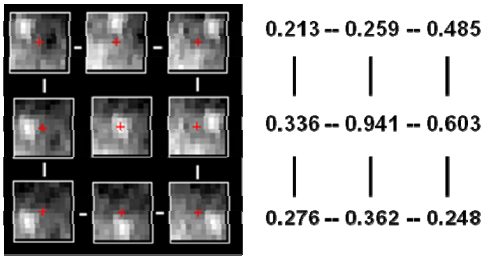

Fig. 6 The output values of the ANN in Fig. 2 corresponding to the input ROIs with different located microcalcifications.

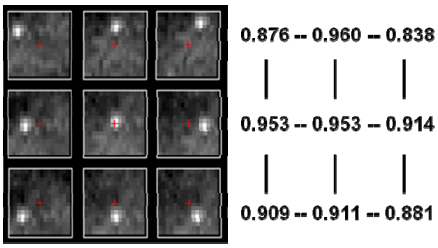

Fig. 7 The output values of FFT-ANN corresponding to the input ROIs with different located microcalcifications.

lower than the threshold that leads to be regarded as FP, as shown in Fig. 6. It is not strange that such ANN could not work well in case of the shifting position of microcalcification, because it did not learn these patterns in the training datasets. If we change the inputs into the power spectra shown in Fig. 3, the result indicates that the output value of ANN changes only a little as shown in Fig. 7. This is due to the fact that the power spectra of a microcalcification has lost the location information in the frequency domain and been centralized at the original point.

For the detection of microcalcification by the ANN in Fig. 4, the location of a single microcalcification could be detected properly with a sensitive rate of detecting TP at 86%. Nevertheless, this structured ANN fails to detect the CMs even if it is in the training procedure. Although it is able to learn a single microcalcification at a random place, the combination of more than three microcalcifications as a CM is very large, and to prepare all these combinations in training datasets is impossible. The same phenomenon can

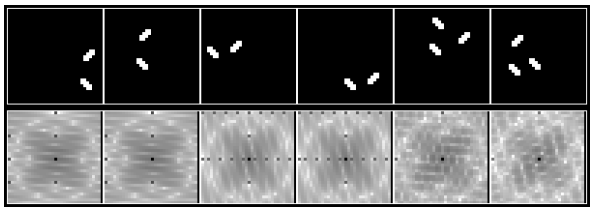

Fig. 8 A training samples of FFT-ANN by transferring the spatial signals to power spectra.

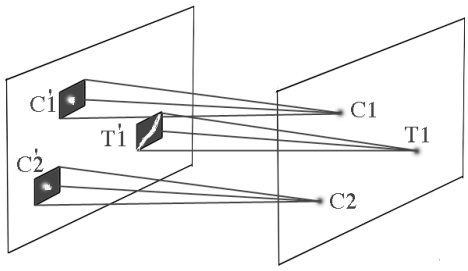

Fig. 9 The interconnection between two groups in two layers. C1, C2 and T1 are disconnected each other.

happen in the frequency domain and the FFT-ANN in Fig. 3 can successfully learn a limited number of teaching samples and detect the CMs correctly which are not included in the training datasets. This is due to the centralization effect of FFT on the power spectra and it can centralize every microcalcification at different locations into the original point. As shown in Fig. 8, the different combinations of two microcalcifications at the upper side have the same power spectra at the lower side. That is why we can train the network with limited examples to detect the clusters which are in the category invariant, rather than requiring the neural network to learn all the gradations of location, shape, size, etc. which are necessary in spatial domain.

SIANN has a spatial architecture but differs from the above full-connected ANN: units in the input layer and output layer corresponding to pixels of the input and output were divided into groups. Every unit in a subsequent layer was connected with the units of a small region called the receptive field in every group in the preceding. In Fig. 9, unit C1 in the subsequent layer received inputs from the receptive field C1' in the preceding layer with black square illustrated. We should notice that the connections of C1 were localized. Therefore, a local variation such as C2 and T1 in the input image did not affect the outputs of the units whose receptive fields did not include the local variation, so the detection of clustered microcalcifications was highly independent of the quantity and position of the microcalcifications. In learning procedure, we can train the SIANN with individual microcalcification C1 and tissue T1 or with clusters C1, C2 and tissue T1 at any place of the input image, which was impossible to a conventional full-connected neural network.

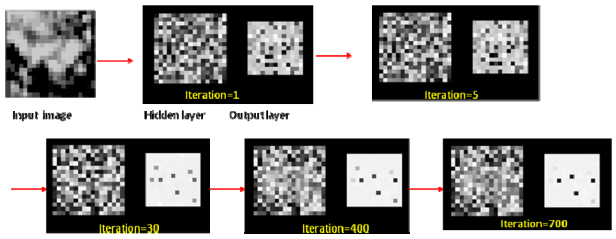

Fig. 10 Illustration of a process of learning in SIANN in different iterations.

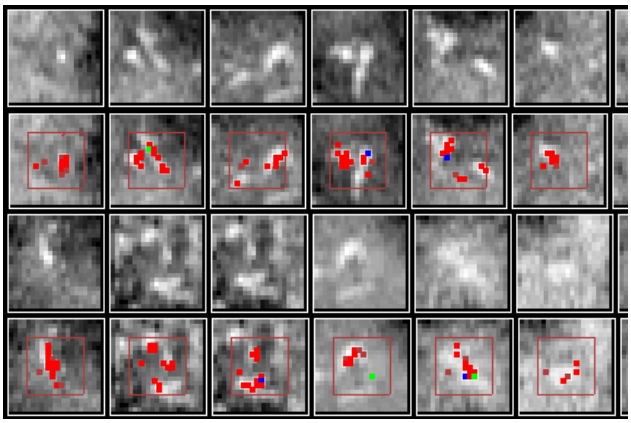

Red: 0.9 ~ 1.0 Blue: 0.8 ~ 0.9 Green: 0.5~ 0.8

Fig. 11 A CMs detection results by SIANN, where the brown square is the size of output layer.

Figure 10 shows a process of learning in SIANN: The network can learn the background very quickly, and then tries to emphasize a foreground teacher signal to black(>0.9) and other foregrounds to white(<0.1) by adjusting the strengths of the connections between the nodes of the network. Cluster training then cluster detecting is the only mode for FFT-ANN to detect CMs. However, we found that single training then cluster detecting mode is also available in SIANN.

Figure 11 shows some CMs detection results by SIANN, where the brown square is the size of output layer. In a practical detection of 30 cases with 40 clusters in masses, 304 out of the whole 537 true microcalcifications were detected by both methods, and the other 61 and 87 of true microcalcifications were detected by TRF and SIANN methods, respectively, with about 120 FP microcalcifications per image. Using both methods, 84% (452/537) of true positives could be picked out. The number of FPs was decreased to 10.2 per image while preserving 432 true positives after using the variable-ring filter. 36 clusters were obtained by the detected microcalcifications from TRF and variable-ring filter, and two other clusters could be found by adding SIANN. Therefore, the sensitivity of detecting clusters was improved from 90% by our previous method to 95% by using both SIANN and TRF with the same number of FPs of 0.85 per image.

IV. CONCLUSIONS

This study demonstrated that the SIANN method was the best ANN to detect clustered microcalcifications. Combining our previous TRF method with SIANN was able to detect 5% additional true clusters compared with the TRF method only, because it detected microcalcifications by learning samples from datasets instead of calculating by explicit mathematical model. Further efficient training has to be done for gaining the potential high generation ability of SIANN. Moreover, it was found that the conventional ANN was also an effective way in eliminating FPs in mass area.

ACKNOWLEDGMENT

This research was supported in part by the National Natural Science Foundations of China (No. 60863014 & 60762001); in part by the Program to Sponsor Teams for Innovation in the Construction of Talent Highlands in Guangxi Institutions of Higher Learning; in part by a research grant of Guangxi University (X071036); in part by a research foundation project of the Guangxi Ministry of Education (No. 200810MS048); and in part by a research grant from the Collaborative Centre for Academy/Industry/Government of Gifu University, the Ministry of Health, Labor, and Welfare under a Grant-In-Aid for Cancer Research, and the Ministry of Education, Culture, Sports, Science and Technology under a Grant-In-Aid for Scientific Research by the Japanese Government.

REFERENCES

[1] J. Harris, M. Lippman, U. Veronesi, et al., "Breast cancer," *N. Engl. J. Med.* **327**, pp. 319-328, 1992.

[2] K. Doi, M. Giger, R. Nishikawa, et al:, "Computer-aided diagnosis of breast cancer on mammograms, " *Breast Cancer* **4**, pp. 228-233, 1997.

[3] K. Hirako, H. Fujita, T. Hara, et al., "Detection scheme for clustered microcalcifications with newly introduced contrast correction technique and variable-ring filter analysis, " *Med. Imag. Tech.* **14**, pp. 665-679, 1996.

[4] K. Hirako, H. Fujita, T. Hara, et al., "Development of detection filter for microcalcifications on mammograms: A method based on density gradient and triple-ring filter analysis," *Trans. Inst. Electron. Inform. Commun. Eng.* **J78-D-II**, pp. 1334-1335, 1995.

[5] K. Seki, H. Fujita, K. Hirako, et al., "Detection of microcalcifications on mammograms using neural networks," *Med. Imag. Tech.* **15**, pp. 639-651, 1997.

[6] W. Zhang, K. Doi, ML. Giger, et al., "An improved shift-invariant artificial neural network for computerized detection of clustered microcalcifications in digital mammograms," *Med. Phys*. **23**, pp. 595-601, 1996.

[7] F. Schwenker, H. A. Kestler, and G. Palm. "Three learning phases for radial-basis-function networks". *Neural Networks*, 14(4-5):439-458, 2001.

[8] J. Moody and C. J. Darken, "Fast learning in networks of locally tuned processing units," *Neural Computation*, 1, 281-294 (1989).

[9] Rumelhart D, McClellend J. "Learning representations by back-propagating errors". *Nature*, 1986; 323: 533-536.

[10] M. Matsubara, H. Fujita, T. Hara, et al., "New algorithm for mass detection in digital mammograms," *Proc. of the 12th International Symposium and Exhibition on Computer Assisted Radiology and Surgery (CAR'98)*, pp. 219-223, 1998.

[11] H. Kato, M. Kanematsu, X. Zhang,etc., "Computer-Aided Diagnosis of Hepatic Fibrosis: Preliminary Evaluation of MRI Texture Analysis Using the Finite Difference Method and an Artificial Neural Network", *American Roentgen Ray Society (AJR)*,vol.189, pp.117-122, 2007

[12] X. Zhang, M. Kanematsu2, H. Fujita3, etc., "Application of an artificial neural network to the computer-aided differentiation of focal liver disease in MR imaging", *Radiological Physics and Technology*, Springer, ISSN 1865-0341, 2009

[13] K. Fukushima: "Neocognitron: A hierarchical neural network capable of visual pattern recognition", *Neural Networks*, **1**[2], pp. 119-130, 1988.